Int. J. Radiation Oncology Biol. Phys., Vol. 67, No. 4, pp. 1248–1258, 2007

0360-3016/07/$–see front matter

doi:10.1016/j.ijrobp.2006.11.036

PHYSICS CONTRIBUTION

DIRECT APERTURE OPTIMIZATION–BASED INTENSITY-MODULATED RADIOTHERAPY FOR WHOLE BREAST IRRADIATION

Ergun E. Ahunbay, Ph.D., Guang-Pei Chen, Ph.D., Steven Thatcher, M.D., Paul A. Jursinic, Ph.D., Julia White, M.D., Katherine Albano, M.S., and X. Allen Li, Ph.D.

Department of Radiation Oncology, Medical College of Wisconsin, Milwaukee, WI

Purpose: To investigate the technical and dosimetric advantages and the efficacy of direct aperture optimized intensity-modulated radiation therapy (DAO-IMRT) over standard (*e.g.*, beamlet optimized) IMRT and conventional three-dimensional conformal radiotherapy (3D-CRT) for whole breast irradiation in supine and prone positions.

Methods and Materials: We retrospectively designed DAO-IMRT plans for 15 breast cancer patients in supine (10 patients) and prone (5 patients) positions with a goal of uniform dose coverage of the whole breast. These DAO-IMRT plans were compared with standard IMRT using beamlet optimization and conventional 3D-CRT plans using wedges. All plans used opposed tangential beam arrangements.

Results: In all cases, the DAO-IMRT plans were equal to or better than those generated with 3D-CRT and standard beamlet-IMRT. For supine cases, DAO-IMRT provided higher uniformity index (UI, defined as the ratio of the dose to 95% of breast volume to the maximum dose) than either 3D-CRT (0.88 vs. 0.82; $p = 0.026$) or beamlet-IMRT (0.89 vs. 0.85; $p = 0.003$). Direct aperture optimized IMRT also gave lower lung doses than either 3D-CRT (V20 = 7.9% vs. 8.6%; $p = 0.024$) or beamlet-IMRT (V20 = 8.4% vs. 9.7%; $p = 0.0008$) for supine patients. For prone patients, DAO-IMRT provided higher UI than either 3D-CRT (0.89 vs. 0.83; $p = 0.027$) or beamlet-IMRT (0.89 vs. 0.85; $p = 0.003$). The planning time for DAO-IMRT was approximately 75% less than that of 3D-CRT. The monitor units for DAO-IMRT were approximately 60% less than those of beamlet-IMRT.

Conclusion: Direct aperture optimized IMRT improved the overall quality of dose distributions as well as the planning and delivery efficiency for treating whole breast in both supine and prone positions. © 2007 Elsevier Inc.

Breast, Direct aperture optimization, IMRT, Segmentation methods, Step-and-shoot.

INTRODUCTION

Conservative surgery with radiotherapy has been established as an alternative to mastectomy for the management of early-stage breast cancer. Traditionally, tangential beam arrangements have been used to deliver breast treatments because no other beam arrangement yielded significant improvement (1). The conventional tangential (two-dimensional [2D]) technique uses proper selection of wedge and beam energy based on a single central axis isodose distribution (2). Although high local control can be achieved (3–5), it results in large hot spots and dose nonuniformities in the breast tissue, especially for large-breasted women. It has been shown that excessive hot spots in the patient results in poorer cosmetic outcome (6–10); therefore, it is desirable to achieve a uniform dose distribution inside the overall breast volume with minimal hot spot regions. The major challenge to improving dose uniformity is the irregular shape and separations of the external contour of the breast. Wedges generate one-directional gradients in the fluence, and therefore multiple wedge angles and directions can only approximate the required intensity variation. Also, to adequately spare the critical structures of the lung and heart, a combination of intensity maps and weights for each beam needs to be created to achieve both objectives. Because there are only two beam angles, it is still possible to find an appropriate combination of wedged beams to get acceptable dose distributions by a human trial-and-error method. However, such a method can be very time consuming and requires a significant amount of resources.

Various groups have studied the potential advantages of intensity-modulated radiotherapy (IMRT) for breast treat-

Reprint requests to: Ergun E. Ahunbay, Ph.D., Department of Radiation Oncology, Medical College of Wisconsin, 9200 W. Wisconsin Ave., Milwaukee, WI 53226. Tel: (414) 805-7898; Fax: (414) 805-4354; E-mail: eahunbay@radonc.mcw.edu

Presented in part at the Annual Meeting of the American Association of Physicists in Medicine, July 24–28, 2005, Seattle, WA.

Supported in part by the Susan Komen Breast Cancer Foundation.

Conflict of interest: none.

Received Aug 9, 2006 and in revised form Nov 1, 2006. Accepted for publication Nov 3, 2006.

ments compared with standard three-dimensional (3D) planning methods (11–19). Most of these studies reported various degrees of dosimetric improvement from IMRT when compared with 3D conformal radiotherapy (3D-CRT) plans using a single wedge-pair. In our institution, the 3D-CRT technique used for breast is complex, involving multiple high- and low-energy beams with a combination of different wedge angles and wedge–gradient directions. In some cases, a field-in-field technique has to be used to achieve desired dose uniformity. Plans generated by this type of 3D-CRT are superior to 2D plans and can be as good as those generated by IMRT, as seen in a separate study by our group (20), in which the comparison results did not show a statistically significant gain for whole breast irradiation with the use of the IMRT in either breast dose uniformity or critical structure sparing. It was noted in the study that the planning time required for IMRT was approximately 75% shorter than that required for 3D-CRT planning.

Most of the previous IMRT breast studies were done with beamlet-based inverse planning methods (11–20), whereby the optimization algorithm optimizes the intensities of finite-sized pencil beams (beamlets) that make up each treatment beam irradiating the patient. A leaf-sequencing algorithm then translates the intensity "map" into segmented fields that can be delivered by a multileaf collimator (MLC) (21–24). Although it is the most widely used approach to IMRT, this method has limitations. The segmentation usually results in too many small segments that require large monitor units. This means a large leakage dose to the patient, long treatment time, and increased maintenance costs for the MLCs. In addition, dosimetry of the plan is compromised by the segmentation process, owing to the restrictions on the number of intensity levels set by the user and machine-specific limitations on MLCs.

In this work, we used a different IMRT optimization algorithm, direct aperture optimization (DAO), to plan IMRT for breast patients in both supine and prone positions. Direct aperture optimization IMRT is an IMRT method in which the aperture shapes and aperture weights are optimized simultaneously, and the MLC constraints and the number of segments are directly included in the optimization process (25). In DAO-IMRT planning, the planner specifies the planning objectives on the basis of the dose–volume criteria for the target and critical structures as well as the number of beam segments to be delivered. The optimization only considers aperture shapes that satisfy the conditions set by the MLC. As a result, high-quality DAO-IMRT treatment plans can be generated using fewer segments (apertures) per beam.

We investigated the dosimetric and technical differences in using DAO-IMRT for breast, retrospectively, on 10 supine and 5 prone breast patients who were previously treated with 3D-CRT (20). We also compared DAO-IMRT plans with standard beamlet-IMRT plans on those patients in terms of dosimetry, number of segments, and monitor units. We compared the quality of treatment plans according to dose uniformity in breast volume, dose uniformity in the irradiated volume, and dose to the surrounding normal tissues of heart and lung.

METHODS AND MATERIALS

Planning systems

We used the XiO CMS treatment-planning system (Computerized Medical Systems, St. Louis, MO) for all the 3D-CRT and beamlet-IMRT planning and the Prowess Panther planning system (Prowess, Chico, CA) for our DAO-IMRT planning. (Note that other commercial planning systems, *e.g.*, Pinnacle (Phillips Medical Systems, Bothell, WA), can also offer DAO-based IMRT.) All planning methods used beam parameters of Siemens MD and Primus machines, with 29 MLCs and virtual wedge.

Both the XiO and Prowess treatment-planning systems use convolution-based dose calculation algorithms. To examine the difference in dose calculations for these two systems, a series of MLC shapes were imported into these two systems for dose calculation. It was found that the dose distributions calculated by the two systems agreed with each other for depths beyond d_{max} (depth of the maximum dose). For doses in the build-up region, a noticeable difference was seen between the two systems. The possible reason for the difference is that the electron contamination is modeled differently in the two dose calculation engines. Nevertheless, this difference should not significantly affect the present dose comparison because we are mainly interested in the dose beyond the build-up region.

Patients

A total of 15 breast cancer patient cases, 10 supine and 5 prone, were studied. The supine group consists of 6 right breast and 4 left breast, with an average breast volume of 1,183 cm^3 (standard deviation [SD] ± 351 cm^3). The prone group consists of 3 right breast and 2 left breast, with an average breast volume of 1,433 cm^3 (SD ± 549 cm^3). Actual treatments for all 15 cases were carried out with the 3D-CRT plans.

Definition of target volumes and critical structures

For each of the 3D-CRT plans, the target breast volume (TBV), ipsilateral lung, and heart (left-sided cases) had been previously contoured. For the purposes of this study, the contralateral lung and contralateral breast were also contoured. At our institution the TBV is a "best fit" that is influenced by the following: clinical borders of the breast defined with wires at time of CT, the contour of the breast volume as it appears on CT, and the location of the lumpectomy cavity on CT. The TBV is designed to encompass the lumpectomy cavity plus a 1.5-cm margin, and it is typically bounded posteriorly by the pectoralis/chest wall muscles and anteriorly by skin.

All volumes used for dose–volume histogram (DVH) analysis for all three planning modalities were identical. For cases in which the TBV contour was at or close to the skin, a second contour was created such that a margin of 5 mm remained between the skin edge and this 5TBV contour. Once modified, the 5TBV was used for all three planning techniques for DVH analysis. Use of the 5TBV as the target volume in IMRT optimizations prevented the IMRT algorithm from putting excessive radiation fluence into the surface of the patient.

Table 1. Results for comparison set 1, between DAO-IMRT and 3D-CRT, on 10 supine patients

	UI		UIG		V20-Lung		V25-Heart		$V_{110\%}$ (cm^3)	
Patient	DAO-IMRT	3D-CRT	DAO-IMRT	3D-CRT	DAO-IMRT	3D-CRT	DAO-IMRT	3D-CRT	DAO-IMRT	3D-CRT
1	0.85	0.79	0.82	0.79	6.7	6.9			0	0
2	0.89	0.88	0.87	0.86	11.1	13.2	9.9	16.3	5	2
3	0.88	0.66	0.86	0.64	5.6	6.2	0.0	0.0	0	6
4	0.89	0.82	0.88	0.82	6.4	6.5			0	4
5	0.88	0.88	0.85	0.85	7.8	8.7	1.4	1.5	13	1
6	0.88	0.86	0.88	0.84	6.2	6.3			1	70
7	0.84	0.82	0.82	0.82	6.6	6.9			27	46
8	0.92	0.88	0.91	0.88	12.3	12.5			0	0
9	0.94	0.77	0.91	0.77	11.7	13.6	4.3	4.3	0	23
10	0.89	0.87	0.87	0.86	5.2	5.3			0	0
Average	0.88	0.82	0.87	0.81	7.9	8.6	5.2	7.4	5	15
p value	0.026		0.036		0.024		0.414		0.179	

Abbreviations: DAO-IMRT = direct aperture optimized intensity-modulated radiotherapy; 3D-CRT = 3-dimensional conformal radiotherapy; UI = uniformity index (ratio of dose that covers 95% of breast volume to maximum breast dose); UIG = global uniformity index (ratio of dose that covers 95% of breast volume to maximum dose in patient); V20-Lung = percentage of lung volume receiving >20 Gy; V25-Heart = percentage of heart volume receiving >25 Gy; $V_{110\%}$ (cm^3) = breast volume that receives >110% of the prescription dose.

Patients 2, 3, 5. and 9 have tumors in left breast, and the V25-heart statistics are done on 3 patients' numbers.

Planning objectives and plan details

All plans were only for uniform whole breast irradiation without the inclusion of the boost dose. None of the treatments included axillary, supraclavicular fossa, or internal mammary chain (IMC) fields. These were the planning parameters for the 3D-CRT plans that were used for actual treatments, and we kept them the same for the other retrospective plans to eliminate any irrelevant differences to affect comparisons. The volumes and contours used for evaluation of the plans for all planning methods were also kept the same. All plans used two tangential beam directions (3D plans having multiple beams coming from the same gantry angle), and no noncoplanar beams were used.

Objectives for the original 3D-CRT plans were based on the criteria of acceptance at our clinic, and they were kept the same for all plans. All plan objectives were based on these criteria: (*1*) cover at least 90% of the TBV with 45 Gy, which is 90% of the prescription dose, (*2*) keep the amount of volume of the TBV at 55 Gy, which is 110% of the prescribed dose, close to zero, (*3*) have <10% of the lung volume receive 20 Gy, and (*4*) have <5% of the heart volume receive 25 Gy, which is 50% of the prescribed dose. All beams excluded the contralateral breast from the irradiated volume.

The 3D-CRT plans for the supine group used two to six different beams with various combinations of heel–anterior, heel–inferior, and heel–superior wedges, 15°–60° wedge angles, and 6-MV, 15-MV and 23-MV beam energies. Multileaf collimator shaped ports and collimator rotation were used to shield the lung and heart. Wedge angles and beam weights and beam energies were chosen to give conformal, homogeneous dose distributions that met the prescription requirements. Isocenter placement varied depending on the position that accomplished the best dose distribution. However, it was usually one third of the distance from the chest wall to the skin in the anterior direction and centered in the medial–lateral direction.

The DAO-IMRT and beamlet-IMRT plans used only 6-MV beams. Uniformity of dose within the TBV, the maximum dose and dose–volume constraints to critical structures were used for the optimization. As in the 3D-CRT plans, no corrections were made for target motion. The dose calculations for all plans were done without tissue heterogeneity corrections. This can be justified because the two planning systems, CMS and Prowess, use different dose algorithms for heterogeneity corrections. To avoid any unfairness in the comparison, the heterogeneity correction was not considered. However, an attempt was made to see the effect if the heterogeneity correction was included. We have generated plans for selected cases with and without heterogeneity correction for the same planning goals. It was found that the difference between the 3D-CRT, DAO-IMRT, and beamlet-IMRT plans was not significantly changed if the heterogeneity correction was turned on, although the dose distributions were different. The heterogeneity-corrected and -uncorrected IMRT plans were very similar in terms of how well the planning objectives were met, indicating that the capabilities of finding a solution to meet the dosimetric criteria in these two systems were not affected when using the heterogeneity correction.

Direct aperture optimized IMRT plans had an open flash field that delivers 70% of the dose to the breast. This field covers the whole breast volume plus a 1–2-cm flash around it in the anterior direction. The rest of the dose is delivered with multiple smaller segments. The leaves in these subsequent segments are limited by the outer boundaries of the initial large "flash" segment, thus the further segments are smaller apertures that are totally inside the initial large segment. Direct aperture optimized IMRT beams all had four to six segments per beam, including the initial flash field, because it was the constraint set during the optimization process.

Comparisons and statistical analysis

Dosimetric comparisons of supine plans were done based on four parameters extracted from DVHs: Uniformity Index (UI), Global Uniformity Index (UIG), V20-lung (fraction of lung volume receiving >20 Gy), and V25-heart (fraction of heart volume receiving >25 Gy). Comparisons of prone plans were done based on only UI and UIG because lung and heart did not receive a significant dose in a prone setting. Following is a brief explanation of these four parameters.

Table 2. Results for comparison set 2, between DAO-IMRT and beamlet-IMRT, on 10 supine patients

	UI		UIG		V20-Lung		V25-Heart		$V_{110\%}$ (cm^3)	
Patient	DAO-IMRT	Beamlet-IMRT	DAO-IMRT	Beamlet-IMRT	DAO-IMRT	Beamlet-IMRT	DAO-IMRT	Beamlet-IMRT	DAO-IMRT	Beamlet-IMRT
1	0.88	0.86	0.86	0.86	9.85	10.5	0	0	0	0
2	0.89	0.88	0.87	0.88	11.05	13.7	9.9	25.1	5	11
3	0.88	0.85	0.86	0.82	4.1	5		0	0	41
4	0.90	0.87	0.89	0.87	9.4	11.1	0	0	0	1
5	0.88	0.85	0.85	0.84	7.8	9.2	1.4	2	13	36
6	0.88	0.86	0.88	0.86	6.5	6.5	0	0	4	20
7	0.84	0.84	0.83	0.79	7.3	8.9	0	0	25	12
8	0.92	0.88	0.91	0.88	12.3	13.7			0	0
9	0.94	0.85	0.91	0.85	11.7	13.8	4.3	18	0	1
10	0.87	0.79	0.86	0.79	4.3	4.6	0	0	0	0
Average	0.89	0.85	0.87	0.84	8.43	9.7	5.2	15.0	5	12
p value	0.003		0.005		0.0008		0.168		0.157	

Abbreviations as in Table 1.

Uniformity Index is defined as $d95/d_{max}$, where d95 is the dose that covers 95% of the breast volume and d_{max} is the maximum dose within the breast volume that covers 4 cm^3 of tissue. We defined UIG as $d95/g_{max}$, where g_{max} is the global maximum (*i.e.*, maximum dose within the patient that covers 4 cm^3 of tissue). Maximum doses that cover at least 4 cm^3 of tissue are used for d_{max} and g_{max} to prevent situations in which the maximum dose represents a very tiny volume with no clinical significance (26). Uniformity Index and UIG are normalized parameters that define the breast dose uniformity and coverage independent of the prescription dose or how the plan dose is scaled. When a plan has a higher UI compared with another plan, it means the dose to breast is more uniform, and when it has a higher UIG, it means either the coverage dose is higher with the same global maximum dose or it has a lower global maximum dose to achieve the same coverage. The UIG can be viewed as the UI of the irradiated volume; it would be equal to UI if the global maximum occurs inside the breast volume and would be lower than UI otherwise.

For supine breast plan comparisons, we also used V20-lung and V25-heart along with UI and UIG. Because the breast volume in the supine setting always overlaps from any beam angle with the lung and heart volumes, the sparing that needs to be achieved will be in tradeoff with the uniformity and coverage of the breast volume; therefore, the UI and UIG parameters will be dependent on V20-lung and V25-heart. The V20-lung and V25-heart parameters are dependent (although very slightly) on the absolute prescription dose (*i.e.*, scaling of the plan); therefore, we defined a fixed scaling method to obtain the V20-lung and V25-heart parameters from a plan such that these parameters are for a plan when the plan is scaled to have breast volume coverage at 50.4 Gy (prescription dose for supine patients), equal to that of the 3D-CRT plan for that patient.

We made three sets of comparisons: in the first comparison set, we compared DAO-IMRT plans with 3D-CRT for 10 supine patients, attempting to keep the V20-lung and V25-heart for the DAO-IMRT the same or lower than the 3D-CRT for each patient. In the second set, we compared DAO-IMRT plans with beamlet-IMRT plans for the same 10 supine patients, also with the V20-lung and V25-heart values of the DAO-IMRT plan lower or equal to those of the beamlet-IMRT plan for each patient. We limited the DAO-IMRT plans' V20-lung and V25-heart numbers by those of the compared plan in each set to make a better comparison mainly in UI and UIG. It is possible to generate many different plans with either method on the same patient with various sparing (V20-lung and V25-heart) and uniformity-coverage (UI and UIG) combinations, and any improvement in one set will translate to the degradation of the other. Therefore, for some of the patients for whom V20-lung and V25-heart values from the 3D-CRT plan were quite

Table 3. Results for comparison set 3, between DAO-IMRT and 3D-CRT, on 5 prone patients

	UI			UIG			$V_{110\%}$ (cm^3)		
Patient	DAO-IMRT	3D-CRT	Beamlet-IMRT	DAO-IMRT	3D-CRT	Beamlet-IMRT	DAO-IMRT	3D-CRT	Beamlet-IMRT
1	0.89	0.88	0.84	0.89	0.88	0.84	0	0	8
2	0.86	0.78	0.81	0.86	0.73	0.81	0	1	1
3	0.88	0.80	0.85	0.88	0.80	0.85	2	1	8
4	0.89	0.88	0.88	0.89	0.88	0.87	0	0	5
5	0.91	0.84	0.86	0.91	0.84	0.86	0	0	0
Average	0.89	0.83	0.85	0.89	0.82	0.84	0	0	0
p value, DAO vs. 3D-CRT	0.027			0.047					
p value DAO vs. beamlet-IMRT	0.003			0.002					

Abbreviations as in Table 1.

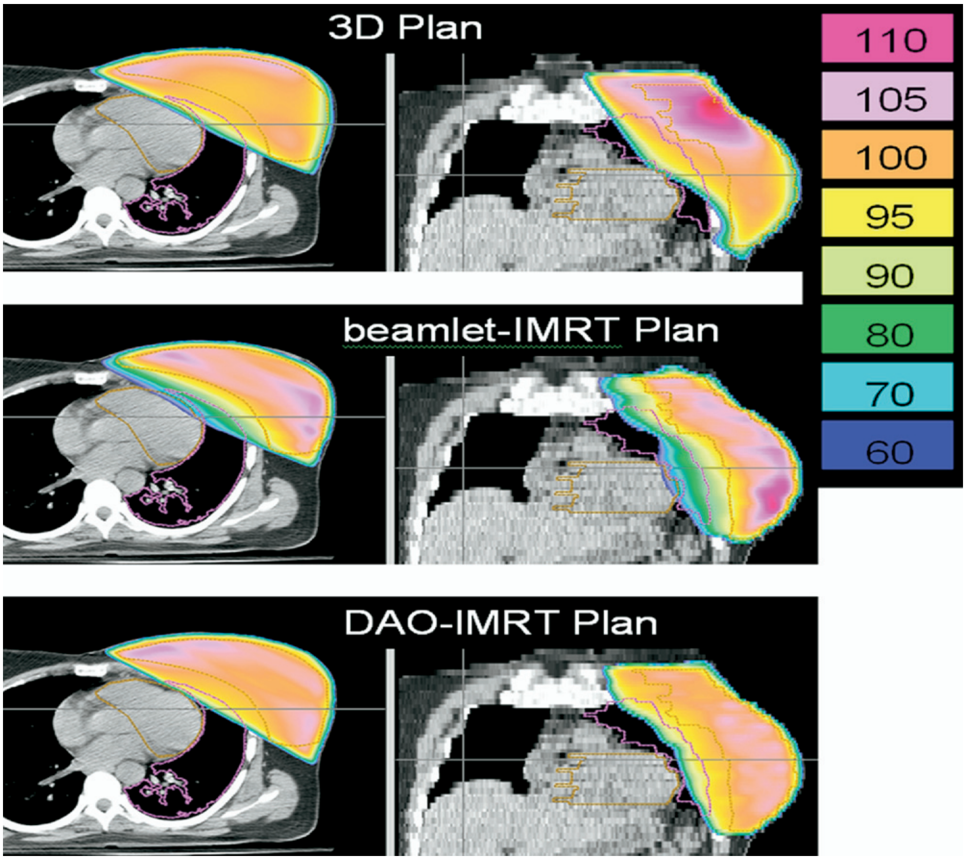

Fig. 1. Transverse and coronal isodose distributions from three-dimensional conformal radiotherapy (3D), beamlet optimized intensity-modulated radiotherapy (beamlet-IMRT), and direct aperture optimized IMRT (DAO-IMRT) plans are shown for a typical left-breast supine case. Figure appears in color online.

different from those of the beamlet-IMRT plan, we generated two separate DAO-IMRT plans to be compared with 3D-CRT and beamlet-IMRT plans.

In the third comparison set, we compared DAO-IMRT plans for 5 prone patients with 3D-CRT and beamlet-IMRT plans. We did not do separate DAO comparisons with 3D-CRT and beamlet-IMRT because there were no compromising V20-lung and V25-heart parameters for prone patients.

The p values for each comparison sets' parameters were calculated with paired Student's t test using Excel (Microsoft, Redmond, WA). We also calculated the mean values and differences in the mean values. Paired Student's t test analyzes two sets of paired data's differences and calculates the probability (p value) that the hypothesis "there is zero difference between the two sets" is true. It is generally accepted that a p value of <0.05 indicates that the difference between the compared parameter sets is statistically significant.

One concern for using IMRT instead of 3D-CRT is whether there is a reduction in skin dose due to the reduced field sizes of IMRT segments. To address this concern, we made surface measurements using thermoluminiscent dosimeter (TLD) chips and a surface diode. For 3 selective cases (1 prone, 2 supine), we delivered one fraction of each of the three planning techniques on a flat phantom. One 3D-CRT plan used physical wedges, whereas the others used virtual wedges. We also made measurements on a RANDO phantom (The Phantom Laboratory, Salem, NY) with new plans generated on this phantom. Whereas the 3D-CRT plans of patient cases had mixed energy beams, for the RANDO phantom we made two separate 3D-CRT plans with only 6-MV and 15-V beams. The monitor units for each plan were normalized to deliver the same fractional dose to breast volume. Only the entrance dose was measured in the flat phantom cases, whereas both exit and entrance doses were measured for RANDO measurement. Flat phantom measurements were performed with gantry angles at 0° and 45°.

RESULTS

Comparison parameters

Data from DVHs were used to extract the UI, UIG, V20-lung, and V25-heart parameters that were explained previously. These data are presented for three sets of comparisons in Tables 1–3.

In Table 1 the first comparison set's results are tabulated. Direct aperture optimized IMRT plans yield superior UI and UIG and equal or lower V20-lung and V25-heart at the same time for each of the 10 supine position cases compared with 3D-CRT plans (average UI = 0.88 vs. 0.82, $p = 0.026$; average V20-lung = 7.9% vs. 8.6%, $p = 0.024$).

The second comparison set's results (between DAO-IMRT and beamlet-IMRT) are listed in Table 2. Direct aperture optimized IMRT shows statistically significant superiority over beamlet-IMRT in both breast dose uniformity and also sparing of the lung and the heart (average UI =

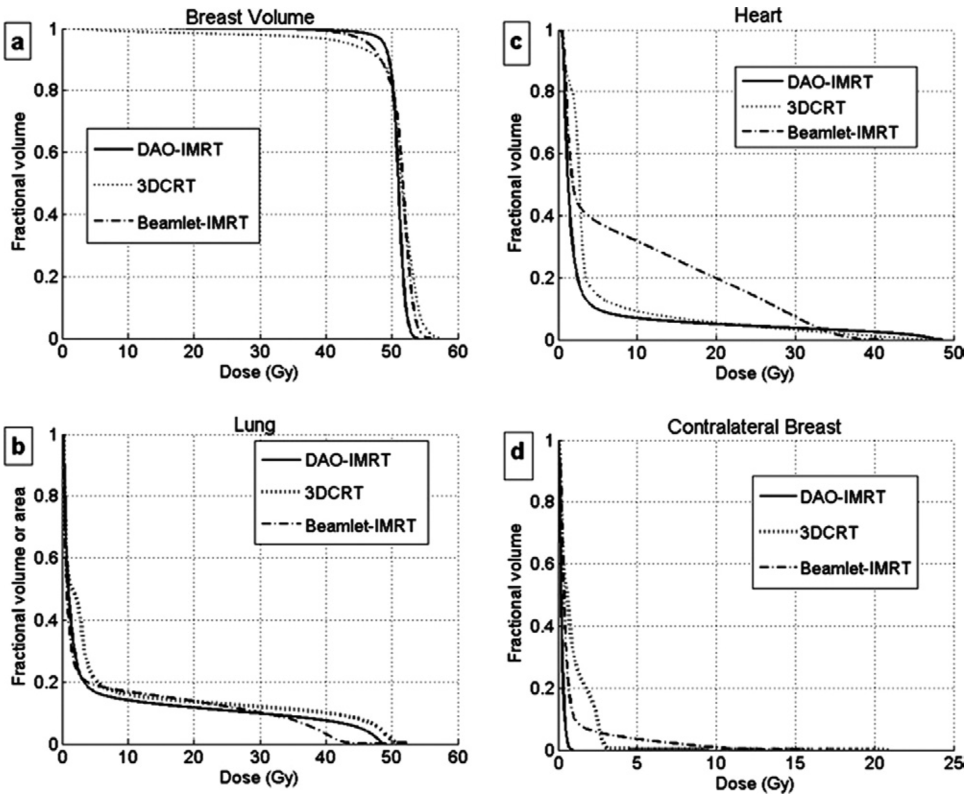

Fig. 2. Dose–volume histograms of the supine patient are shown for (a) breast volume, (b) lung, (c) heart, and (d) contralateral breast. DAO-IMRT = direct aperture optimized intensity-modulated radiotherapy; 3DCRT = three-dimensional conformal radiotherapy.

0.89 vs. 0.85, $p = 0.003$; average V20-lung = 8.4% vs. 9.7%, $p = 0.0008$).

The third comparison set's results are listed in Table 3. For each of the 5 prone patient cases, DAO-IMRT plans yielded better dose uniformity compared with both 3D-CRT and beamlet-IMRT plans (average UI = 0.89 [DAO-IMRT] vs. 0.83 [3D-CRT], $p = 0.027$, and vs. 0.85 [beamlet-IMRT], $p = 0.003$).

To evaluate the effect of using different planning methods on breast cosmesis, we tabulated another parameter, $V_{110\%}$, in Tables 1–3 for all plans; $V_{110\%}$ is the absolute volume that received more than the 110% of the prescription dose. According to one resource (19), cosmetic outcome of whole breast radiotherapy is correlated to whether $V_{110\%}$ exceeds 200 cm^3. In all the plans, this volume is <200 cm^3.

Isodose plots and DVHs

In Fig. 1, isodose distributions from three plans are displayed for a typical supine patient (Patient 9). This is a left-sided breast case with more than 22 cm maximum separation and a breast volume of 1246 cm^3. For this patient a single DAO plan was generated and used for comparison with both the 3D-CRT and beamlet-IMRT plans. For the 3D-CRT plan, three beams with mixed energies of 6 MV and 23 MV were used with 15° heel–anterior wedges. For the beamlet-IMRT plan, two beams with 49 segments were used, whereas for the DAO-IMRT plan six segments per beam were used. The isodoses depicted are for the plans normalized to the same amount of breast volume receiving at least 50.4 Gy prescription dose. At this normalization, DVH plots for important regions of interest are plotted in Fig. 2. Segment shapes of one beam and the resulting intensity maps for beamlet-IMRT and DAO-IMRT are depicted in Fig. 3.

In Fig. 4, isodose distributions from the three planning methods are displayed for a typical prone patient. Dose–volume histogram plots for important regions of interest are plotted in Fig. 5. Direct aperture optimized IMRT delivers a lower dose to the lung and the heart, with a slightly more uniform tumor dose to the breast volume (Fig. 5).

Monitor units and number of segments

Direct aperture optimized IMRT plans use 4–6 segments per beam, whereas beamlet-IMRT plans have a range of 9–39 segments per beam. Beamlet-IMRT monitor units are on the average 60% greater (range, 20–130%) than DAO-IMRT. In Table 4 we listed the number of segments and monitor units used by each method for 14 patients. Patient 3 3D-CRT monitor unit data could not be obtained. Three-dimensional CRT plans using virtual wedges require significantly less monitor units than those using physical wedges. Direct aperture optimized IMRT monitor units are 5–15% greater than those of 3D-CRT plans when a virtual wedge is

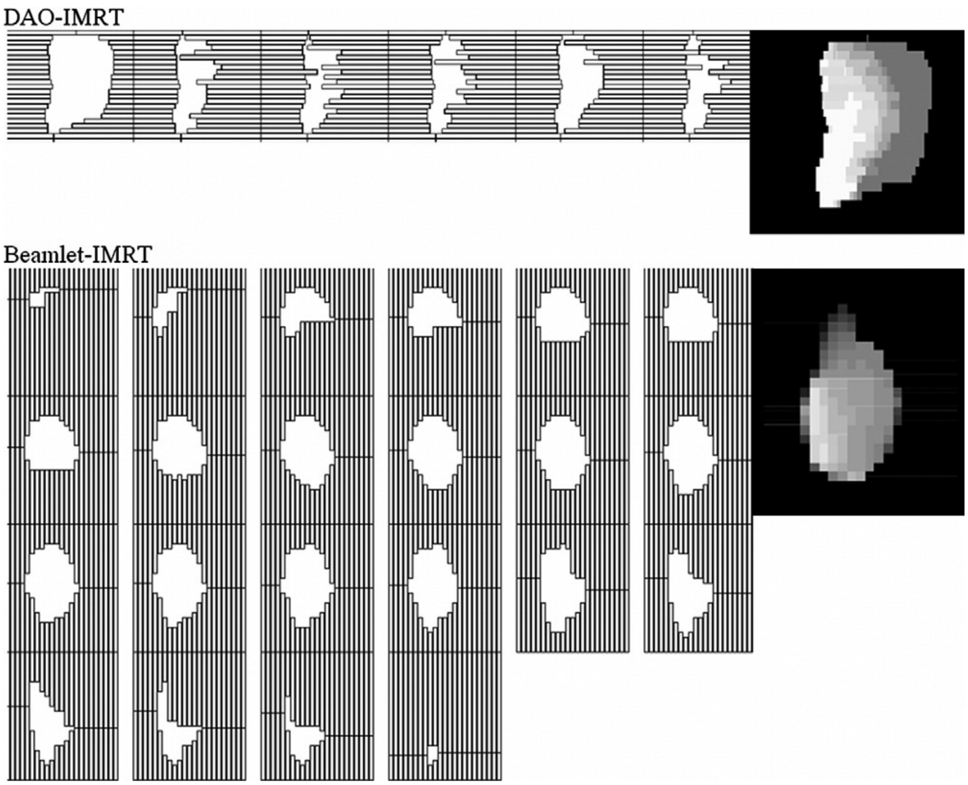

Fig. 3. Shapes of segments and the resulting intensity map for a typical beam direction are shown for both direct aperture optimized intensity-modulated radiotherapy (DAO-IMRT) and beamlet optimized IMRT plans.

used and approximately 30–90% less when a physical wedge is used. In these comparisons, total monitor units to give the total dose of approximately 50.4 Gy to breast volume are divided by 25 fractions for all plans. The monitor units of the DAO-IMRT plans for some supine patients in Table 4 are the average of the two DAO-IMRT plans that were used for comparison sets 1 and 2, and the two numbers for any patient did not differ by more than 1%.

Planning and delivery time

Table 4 shows treatment time estimates for all plans. In these time estimates, the following approximations were used: dose rate, 200 monitor units/min; IMRT segmentation time, 8 s; gantry rotation time from lateral to medial, 30 s; wedge replacement time, 25 s. Our estimates for treatment times are 2.5 min for 3D-CRT, 3.2 min for DAO-IMRT, and 7.1 min for beamlet-IMRT. The Siemens virtual wedge's dose rate decrease (27) was included in these time estimations. For throughput considerations, 3D-CRT and DAO-IMRT treatments fit easily into the 15-min treatment slot, and beamlet-IMRT treatments would require slightly longer treatment slots of 17 min.

Treatment planning time and effort for 3D-CRT plans are significantly greater than for both IMRT methods (60–90 min for 3D-CRT vs. approximately 20 min for either IMRT method). Three-dimensional CRT breast plans require extensive effort by personnel with advanced treatment-planning skills, whereas high-quality IMRT plans can be generated in less time with much less experience in a more automated fashion. For these reasons, there is a higher likelihood of suboptimal plan generation with 3D-CRT compared with IMRT planning. In IMRT, plan implementation requires that IMRT quality assurance be performed for each plan, which in our clinic requires approximately 30 min for a breast plan.

For all the flat phantom measurements, the 3D-CRT plans had lower surface doses than the IMRT plans, by more than 10%. For both the flat phantom and RANDO measurements, the DAO-IMRT plans' surface doses were only slightly higher (2–5%) than beamlet-IMRT plan values, which would be within the uncertainty of our measurements. The lower surface doses for the 3D-CRT plans in our cases are attributed to the use of higher-energy beams. Thus, the necessity of using higher-energy beams to achieve adequate dosimetry may result in lower skin doses for 3D-CRT plans. When only a 6-MV beam was used for the RANDO plan, the skin doses were 9% higher for the 3D-CRT plan compared with the DAO-IMRT plan.

DISCUSSION

The requirement for IMRT for breast radiotherapy originates from the complicated shape of the external contour as well as the proximity of the target to critical structures. Wedges have been used as the standard tool in breast planning; however, they can only generate intensity gradi-

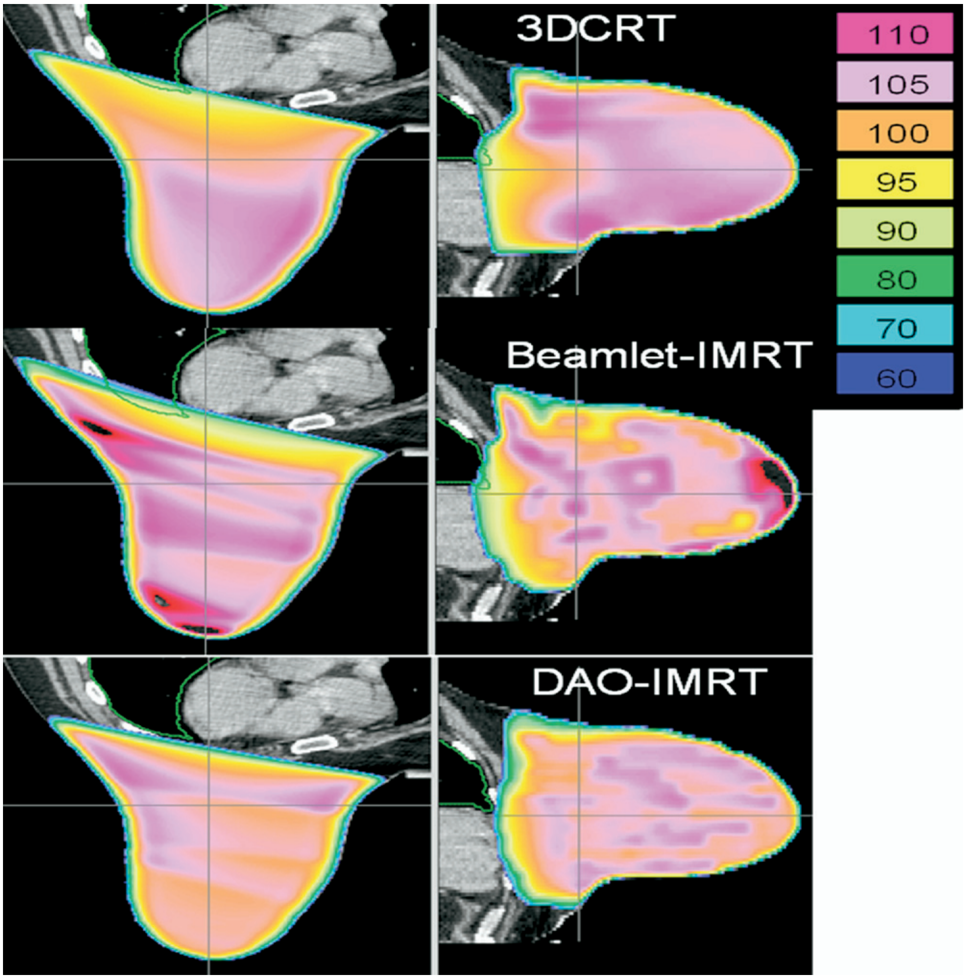

Fig. 4. Transverse and sagittal isodose distributions from three-dimensional conformal radiotherapy (3DCRT), beamlet optimized intensity-modulated radiotherapy (beamlet-IMRT), and direct aperture optimized IMRT (DAO-IMRT) plans are shown for a typical prone case. Figure appears in color online.

ents in a single direction. Compensators with their 2D intensity variation capability have been used for generating a uniform dose in breast; however, they cause large scatter dose to the contralateral breast (28). In addition, compensators without inverse planning do not address the sparing of critical structures as well as the uniformity of breast volume. Intensity-modulated radiotherapy has the capability of generating the 2D intensity maps necessary to meet the uniformity and sparing criteria.

Intensity-modulated radiotherapy planning, when done by means of standard beamlet optimization, does not necessarily generate the most optimum intensity distributions, owing to the degradation of the plan during the segmentation process. In beamlet IMRT, the effect of segmentation is totally ignored during the optimization, and the optimum solution has to be compromised during segmentation unless a large number of segments are used. This makes the quality of the IMRT plans for breast lower than some of the 3D-CRT planning techniques; therefore, the clinical superiority of IMRT over conventional radiotherapy for breast cancer is still debatable.

Advantages of DAO-IMRT have been discussed by other groups (25). In summary, DAO-IMRT offers the possibility of using inverse planning–based optimization with the simplicity of 3D delivery. Therefore, benefits of inverse planning can be exploited while disadvantages of standard beamlet-IMRT are minimized (*e.g.*, longer treatment times, complicated delivery and quality assurance, increased MLC position dependence and MLC maintenance requirement, and increased leakage radiation to the patient). To benefit from these advantages, it needs to be proven that DAO-IMRT is capable of generating dosimetry at least as good as in the standard methods. Direct aperture optimized IMRT might not be as powerful as beamlet-based IMRT for generating intensity maps, especially with high amounts of modulation (peaks and valleys in the intensity map), which typically is required for other sites like prostate or head and neck. Breast IMRT, however, usually does not require highly modulated intensity maps because there are only two beam directions and the main source for intensity variation is the variation in separation thickness around the breast, which is a smoothly varying function seen from the beams-eye-view. In this work, we demonstrate that for whole breast irradiation, there will not be any degradation in

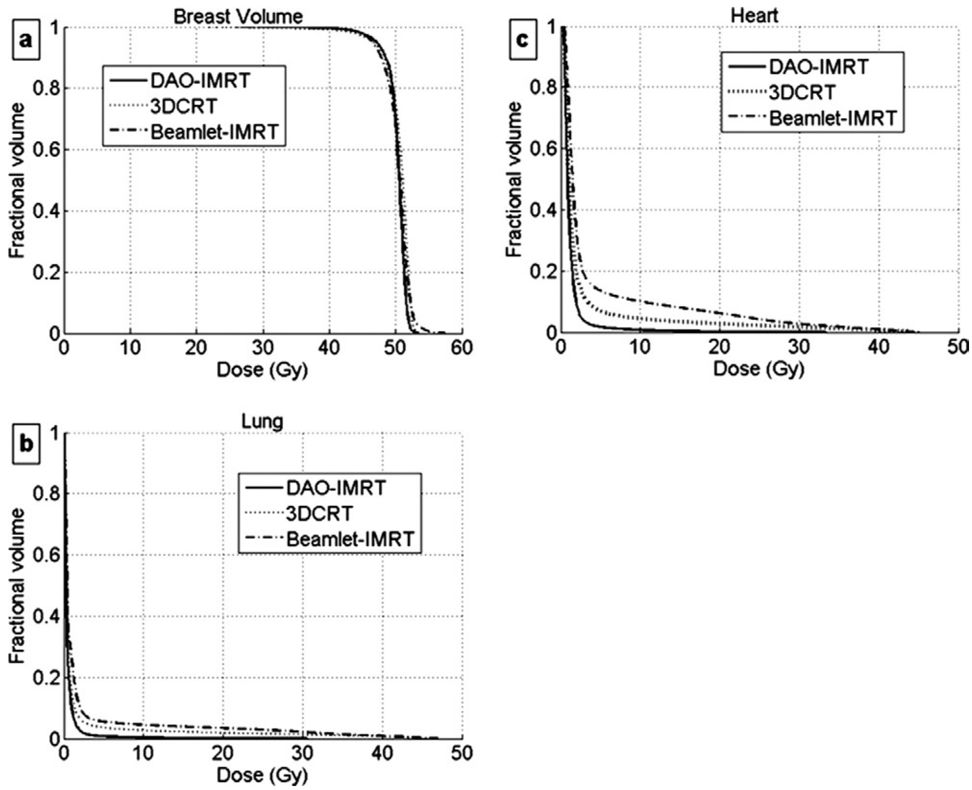

Fig. 5. Dose–volume histograms of the prone patient are shown for (a) breast volume, (b) lung, and (c) heart. DAO-IMRT = direct aperture optimized intensity-modulated radiotherapy; 3DCRT = three-dimensional conformal radiotherapy.

dosimetric quality when DAO-IMRT planning is used instead of standard 3D or IMRT, and probably there will be some improvements in both target dose uniformity and critical organ sparing.

The probability for radiation-induced secondary malignancies may increase when larger volumes of normal tissue are exposed to lower doses (29, 30). The leakage and scatter dose to nontarget tissue of the patients will be proportional to the number of monitor units used. We performed a risk estimate calculation for radiation-induced malignancies, whereby we assumed the whole-body dose equivalent to be 8×10^{-4} Sv/1 Gy (29) and the lifetime risk for fatal secondary cancers to be 5%/Sv (30). We determined the lifetime risk for fatal secondary cancers to be roughly 0.20%, 0.38%, 0.23%, and 0.37%, respectively, for 3D-CRT using virtual wedge, 3D-CRT using physical wedge, DAO-IMRT, and beamlet-IMRT. It should be kept in mind that these risk factors have a high amount of uncertainty because they are based on small numbers of cancers induced in populations exposed to ionizing radiation.

In the present study, we observed a small but statistically significant improvement in both uniformity of breast dose and critical tissue sparing with DAO-IMRT compared with both 3D-CRT and standard IMRT plans for both supine and prone patients. These results are listed in Tables 1–3. For example, the mean UI increases from 0.82 to 0.88 (p = 0.025) for supine breast patients and from 0.83 to 0.89 (p = 0.027) for prone patients when DAO-IMRT is used instead of 3D-CRT. Another parameter, UIG, which is the quotient of the dose that covers 95% of the breast volume to global maximum dose, increases when DAO-IMRT is used for both prone and supine patients compared with other methods. This means that higher tumor doses can be achieved by DAO-IMRT compared with other methods with the same global maximum dose.

An important question is what clinical effect one may expect from these different approaches to treatment planning and delivery. Reports in the literature show various parameters that are correlated to cosmetic outcome. A rapid degradation in cosmetic result occurred when the dose to the whole breast exceeded 65 Gy (9). Many reports (6–9) demonstrate that cosmetic results are poorer in patients with large breast volumes. It was shown (6) that the percentage of breast tissue receiving 110% of the prescribed dose increased with breast volume. It was hypothesized (6) that this higher heterogeneity in dose in large-breasted patients was the cause of poor cosmesis. Taylor *et al.* (9) showed that cosmetic results were poor when dose homogeneity was greater than 108% when dose delivery was made without compensators or wedges in a beam, and Vicini *et al.* (19) demonstrated that acute skin toxicity greatly increased when $V_{110\%}$-breast exceeds 200 cm^3. As Tables 1–3 demonstrate, all of the treatment plans studied here had $V_{110\%}$-breast $<$200 cm^3, and therefore at this prescription level a significant variation in cosmetic outcome due to the selection of different planning methods is not expected.

Table 4. Number of segments/beams, monitor units, and treatment time estimates for each planning method for 10 supine and 5 prone patients

	No. of segments			Monitor units			Treatment time (min)		
Patient	DAO-IMRT	3D-CRT	Beamlet-IMRT	DAO-IMRT	3D-CRT	Beamlet-IMRT	DAO-IMRT	3D-CRT	Beamlet-IMRT
Supine									
1	12	4	40	262	416	306	3.1	2.8	7.4
2	12	6	57	257	385	605	3.9	2.4	11.1
3	12								
4	12	4	37	245	385	336	3.3	2.4	7.1
5	12	6	46	268	363	379	3.4	2.3	8.5
6	12	2	39	257	476	402	3.4	2.9	7.7
7	12	6	60	282	419	622	3.5	2.6	11.6
8	8	3	37	255	208	317	2.8	2.0	7.0
9	12	4	49	245	198	411	3.3	2.1	9.1
10	12	3	33	251	201	345	3.4	2.2	6.6
Prone									
1	8	3	28	234	248	430	2.7	2.4	6.4
2	10	3	22	233	222	347	3.0	2.0	5.2
3	12	3	25	226	210	425	3.2	1.9	6.0
4	10	4	18	228	220	325	3.0	2.0	4.5
5	12	3	20	226	215	361	3.2	1.8	5
Average	11	4	37	248	407* 215†	401	3.2	2.6* 2.1†	7.1
Standard Deviation	1	1	13	17	40*16†	99	0.3	0.2* 0.2†	2.1

Abbreviations as in Table 1.

For supine Patients 1–7, 3D-CRT plans use physical wedges, whereas the rest of the 3D-CRT plans use virtual wedges. The 3D-CRT monitor unit data could not be retrieved for Patient 3. For 3D-CRT plans, the number of segments is the number of separate beams used.

* Physical wedge.

† Virtual wedge.

CONCLUSION

In conclusion, we report that DAO-IMRT can achieve equal or better plans for whole breast irradiation as the complicated 3D-CRT planning with wedges or standard beamlet-IMRT in terms of dose uniformity, critical organ sparing, and maintenance of good cosmetic results. The DAO-IMRT planning is proficient, and the plans can be delivered efficiently because small numbers of segments and monitor units are used.

REFERENCES

1. Solin LJ, Chu JCH, Sontag MR, *et al.* Three-dimensional photon treatment planning of the intact breast. *Int J Radiat Oncol Biol Phys* 1991;21:193–203.
2. Kutcher GJ, Smith AR, Fowble BL, *et al.* Treatment planning for primary breast cancer: A Patterns of Care study. *Int J Radiat Oncol Biol Phys* 1996;36:731–737.
3. Fisher B, Redmond C, Poisson R, *et al.* Eight-year results of a randomized clinical trial comparing total mastectomy, and lumpectomy with or without irradiation in the treatment of breast cancer. *N Engl J Med* 1989;320:822–828.
4. Lingos TI, Recht A, Vicini FA, *et al.* Radiation pneumonitis in breast cancer patients treated with conservative surgery and radiation therapy. *Int J Radiat Oncol Biol Phys* 1991;21:355–360.
5. Wallgren A. Late effects of radiotherapy in the treatment of breast cancer. *Acta Oncol* 1992;31:237–242.
6. Buchholz TA, Gurgoze E, Bice WS, *et al.* Dosimetric analysis of intact breast irradiation in off-axis planes. *Int J Radiat Oncol Biol Phys* 1997;39:261–267.
7. Gray JR, McCormick B, Cox L, *et al.* Primary breast irradiation in large-breasted or heavy women: Analysis of cosmetic outcome. *Int J Radiat Oncol Biol Phys* 1991;21:347–354.
8. Moody AM, Mayles WPM, Bliss JM, *et al.* The influence of breast size on late radiation effects and association with radiotherapy dose inhomogeneity. *Radiother Oncol* 1994;33:106–112.
9. Taylor ME, Perez CA, Halverson KJ, *et al.* Factors influencing cosmetic results after conservation therapy for breast cancer. *Int J Radiat Oncol Biol Phys* 1995;31:753–764.
10. Cheng CW, Das IJ, Baldassarre S. The effect of the number of computed tomographic slices on dose distributions and evaluation of treatment planning systems for radiation therapy of intact breast. *Int J Radiat Oncol Biol Phys* 1994;30:183–195.
11. Mihai A, Rakovitch E, Sixel K, *et al.* Inverse vs. forward breast IMRT planning. *Med Dosim* 2005;30:149–154.
12. Hong L, Hunt M, Chui C, *et al.* Intensity-modulated tangential beam irradiation of the intact breast. *Int J Radiat Oncol Biol Phys* 1999;44:1155–1164.
13. Teh BS, Lu HH, Sobremonte S, *et al.* The potential use of intensity modulated radiotherapy (IMRT) in women with pectus excavatum desiring breast-conserving therapy. *Breast J* 2001;7:233–239.
14. Van Asselen B, Raaijmakers CP, Hofman P, *et al.* An improved breast irradiation technique using three-dimensional geometrical information and intensity modulation. *Radiother Oncol* 2001;58:341–347.

15. Partridge M, Aldridge S, Donovan E, *et al.* An intercomparison of IMRT delivery techniques: A case study for breast treatment. *Phys Med Biol* 2001;46:N175–N185.
16. Hurkmans C, Cho J, Damen E, *et al.* Reduction of cardiac and lung complication probabilities after breast irradiation using conformal radiotherapy with or without intensity modulation. *Radiother Oncol* 2002;62:163–171.
17. Cho BC, Hurkmans CW, Damen EM, *et al.* Intensity modulated versus non-intensity modulated radiotherapy in the treatment of the left breast and upper internal mammary lymph node chain: A comparative planning study. *Radiother Oncol* 2002;62:127–136.
18. Lo YC, Yasuda G, Fitzgerald TJ, *et al.* Intensity modulation for breast treatment using static multi-leaf collimators. *Int J Radiat Oncol Biol Phys* 2000;46:187–194.
19. Vicini FA, Sharpe M, Kestin L, *et al.* Optimizing breast cancer treatment efficacy with intensity-modulated radiotherapy. *Int J Radiat Oncol Biol Phys* 2002;54:1336–1344.
20. Thatcher SH, Jursinic PA, Yun H, *et al.* Comparison of intensity modulated and 3D-conformal treatment breast plans with and without lumpectomy boost [abstract]. *Int J Radiat Oncol Biol Phys* 2004;60:S394.
21. Bortfeld T, Haler DH, Waldron TJ, *et al.* X-ray compensation with multileaf collimators. *Int J Radiat Oncol Biol Phys* 1994;28:723–739.
22. Galvin JM, Chen XG, Smith RM. Combining multileaf field to modulate fluence distributions. *Int J Radiat Oncol Biol Phys* 1993;27:697–705.
23. Webb S. Configuration options for intensity-modulated radiation therapy using multiple static fields shaped by a multileaf collimator. *Phys Med Biol* 1998;43:241–260.
24. Webb S. Configuration options for intensity-modulated radiation therapy using multiple static fields shaped by a multileaf collimator. II: Constraints and limitations on 2D modulation. *Phys Med Biol* 1998;43:1482–1495.
25. Shephard DM, Earl MA, Li XA, *et al.* Direct aperture optimization: A turnkey solution for step-and-shoot IMRT. *Med Phys* 2002;29:1007–1018.
26. International Commission on Radiation Units and Measurements. Prescribing, recording, and reporting photon beam therapy. Report 50. Bethesda, MD: ICRU; 1993.
27. Zhu XR, Gillin MT, Ehlers K, *et al.* Dependence of virtual wedge factor on dose calibration and monitor units. *Med Phys* 2001;28:174–177.
28. Chang SX, Deschesne KM, Cullip TJ, *et al.* A comparison of different intensity modulation treatment techniques for tangential breast irradiation. *Int J Radiat Oncol Biol Phys* 1999;45:1305–1314.
29. Followill D, Geis P, Boyer A. Estimates of whole-body dose equivalent produced by beam intensity modulated conformal therapy. *Int J Radiat Oncol Biol Phys* 1997;38:667–672.
30. Hall EJ, Wuu C. Radiation-induced second cancers: The impact of 3D-CRT and IMRT. *Int J Radiat Oncol Biol Phys* 2003;56:83–88.